

Supporting Information

Halogen-involving weak interactions manifested in the crystal structures of silver(I) or gold(I) 4-halogenated-3,5- diphenylpyrazolato trimers

Jing-Huo Chen^a, Ya-Mei Liu^a, Jin-Xue Zhang^a, Yan-Yan Zhu^a, Ming-Sheng Tang^a,
Seik Weng Ng^{b,c}, Guang Yang^{a}*

^a The College of Chemistry and Molecular Engineering, Zhengzhou University,
Zhengzhou, Henan, 450052, P. R. China

^b Department of Chemistry, University of Malaya, 50603, Kuala Lumpur, Malaysia

^c Chemistry Department, Faculty of Science, King Abdulaziz University,
Jeddah, Saudi Arabia

* To whom correspondence should be addressed. E-mail: Yang@zzu.edu.cn

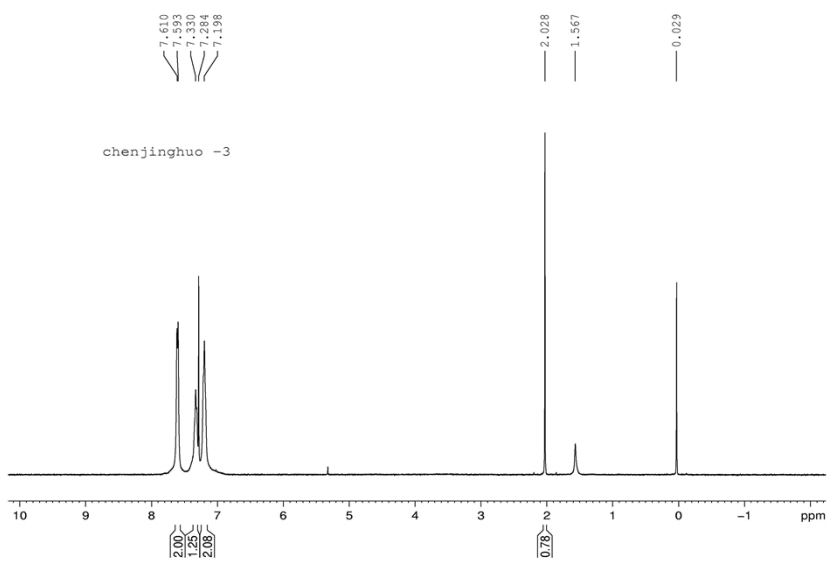


Figure S1a. ^1H NMR spectrum of $[\text{Ag}(\text{ClPh}_2\text{pz})]_3 \cdot \text{CH}_3\text{CN}$ (**1**) in CDCl_3 .

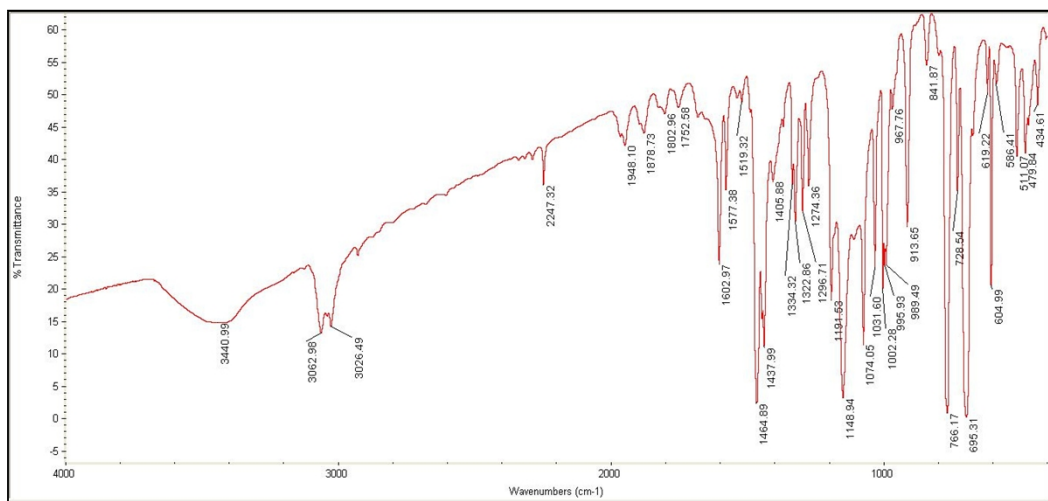


Figure S1b. IR spectrum of $[\text{Ag}(\text{ClPh}_2\text{pz})]_3 \cdot \text{CH}_3\text{CN}$ (**1**) in KBr pellet.

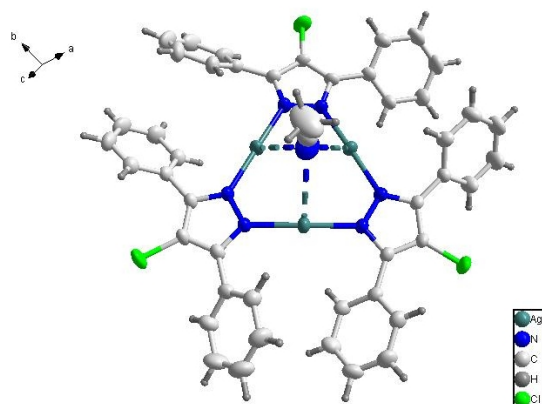


Figure S1c. The asymmetric unit of $[\text{Ag}(\text{ClPh}_2\text{pz})]_3 \cdot \text{CH}_3\text{CN}$ (**1**).

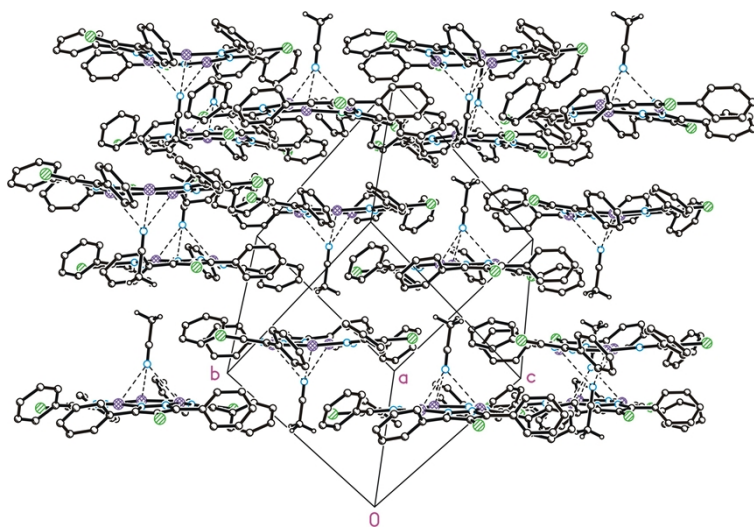


Figure S1d. Packing diagram of $[\text{Ag}(\text{ClPh}_2\text{pz})]_3 \cdot \text{CH}_3\text{CN}$ (**1**).

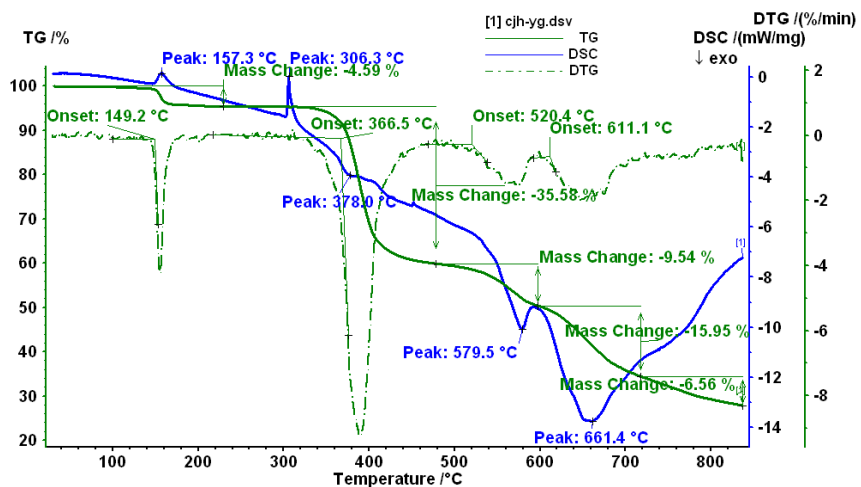


Figure S1f. TG-DSC curves of $[\text{Ag}(\text{ClPh}_2\text{pz})]_3 \cdot \text{CH}_3\text{CN}$ (**1**).

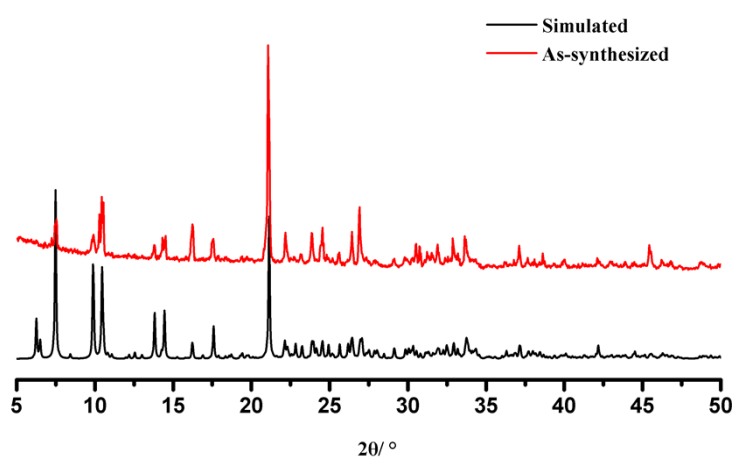


Figure S1g. The PXRD patterns of $[\text{Ag}(\text{ClPh}_2\text{pz})]_3 \cdot \text{CH}_3\text{CN}$ (**1**) obtained from the as-synthesized sample (red line) and the simulation based on the crystal data (black line).

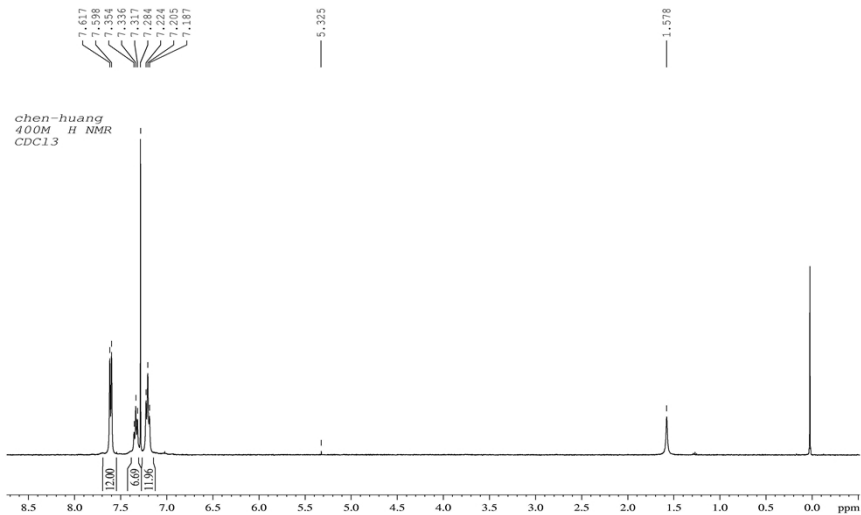


Figure S2a. ^1H NMR spectrum of $[\text{Ag}(\text{ClPh}_2\text{pz})]_3 \cdot 2\text{CH}_2\text{Cl}_2$ (**2**) in CDCl_3 .

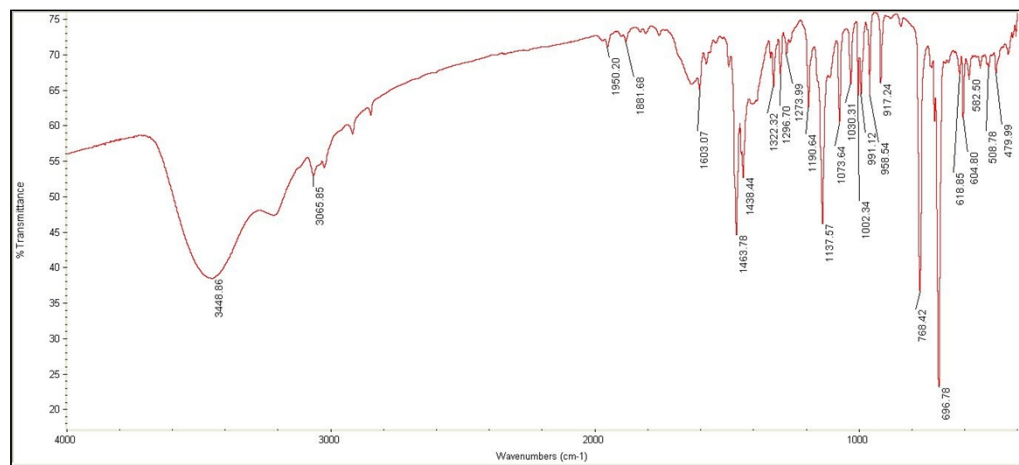


Figure S2b. IR spectrum of $[\text{Ag}(\text{ClPh}_2\text{pz})]_3 \cdot 2\text{CH}_2\text{Cl}_2$ (**2**) in KBr pellet.

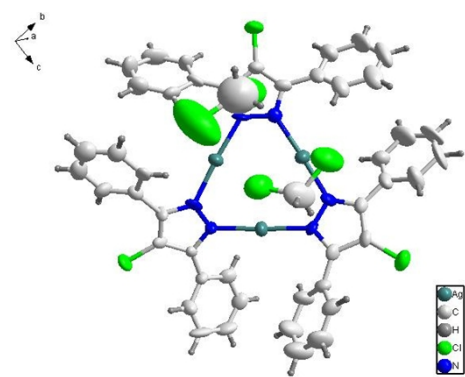


Figure S2c. The asymmetric unit of $[\text{Ag}(\text{ClPh}_2\text{pz})]_3 \cdot 2\text{CH}_2\text{Cl}_2$ (**2**).

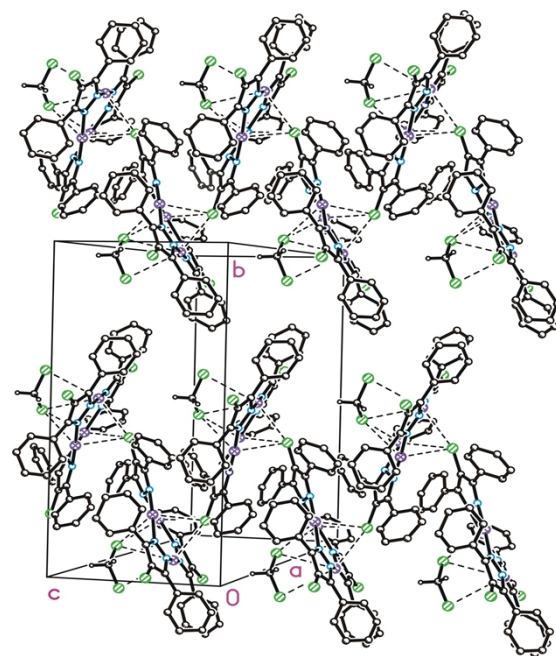


Figure S2d. Packing diagram of $[\text{Ag}(\text{ClPh}_2\text{pz})]_3 \cdot 2\text{CH}_2\text{Cl}_2$ (**2**).

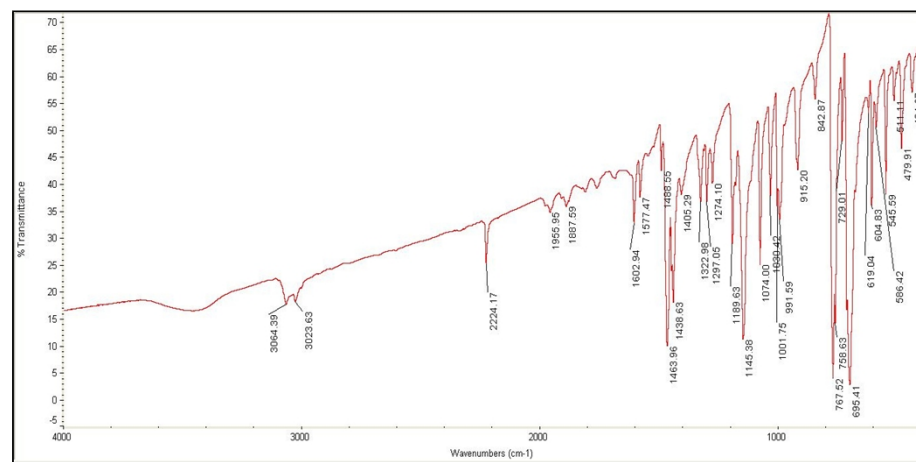


Figure S3a. IR spectrum of $[\text{Ag}(\text{ClPh}_2\text{pz})]_3 \cdot \text{PhCN}$ (**3**) in KBr pellet.

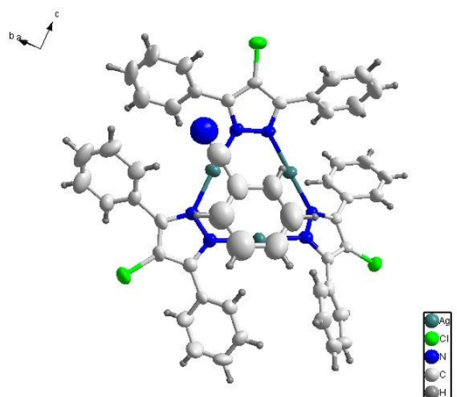


Figure S3b. The asymmetric unit of $[\text{Ag}(\text{ClPh}_2\text{pz})]_3 \cdot \text{PhCN}$ (**3**).

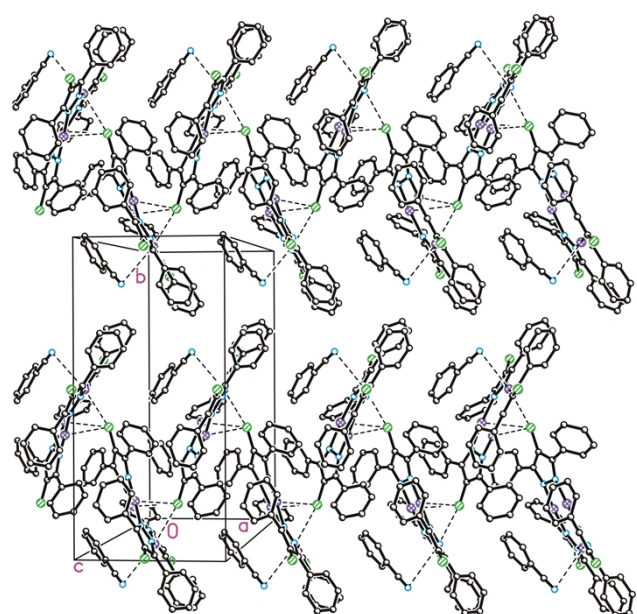


Figure S3c. Packing diagram of $[\text{Ag}(\text{ClPh}_2\text{pz})]_3 \cdot \text{PhCN}$ (**3**).

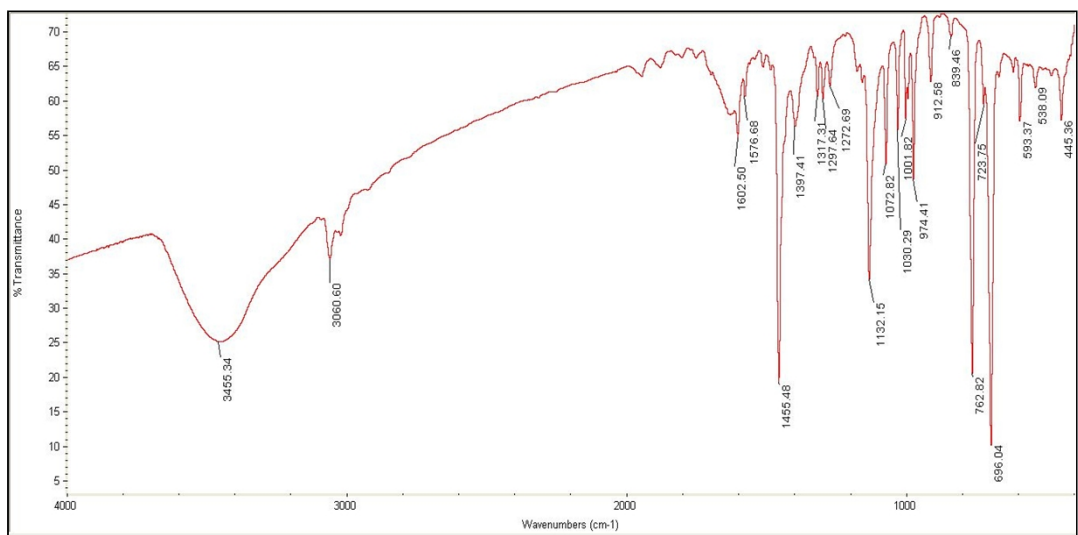


Figure S4a. IR spectrum of $[\text{Ag}(\text{IPh}_2\text{pz})]_3$ (**4**) in KBr pellet.

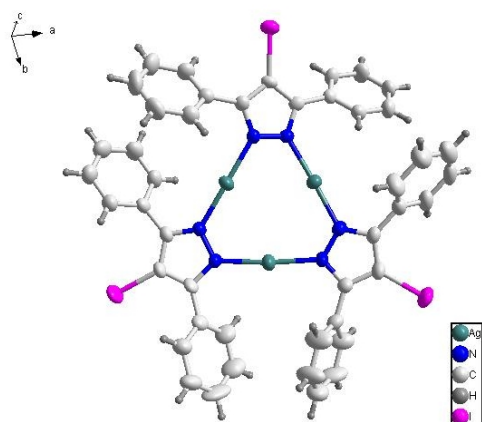


Figure S4b. The asymmetric unit of $[\text{Ag}(\text{IPh}_2\text{pz})]_3$ (**4**).

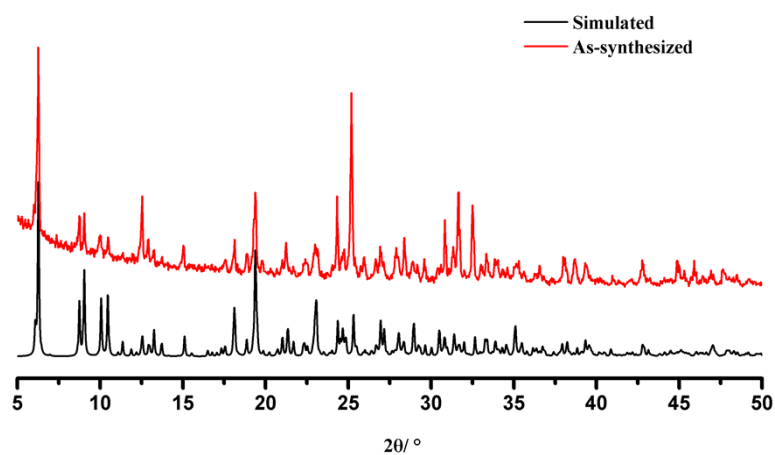


Figure S4c. The PXRD patterns of $[\text{Ag}(\text{IPh}_2\text{pz})]_3$ (**4**) obtained from the as-synthesized sample

(red line) and the simulation based on the crystal data (black line).

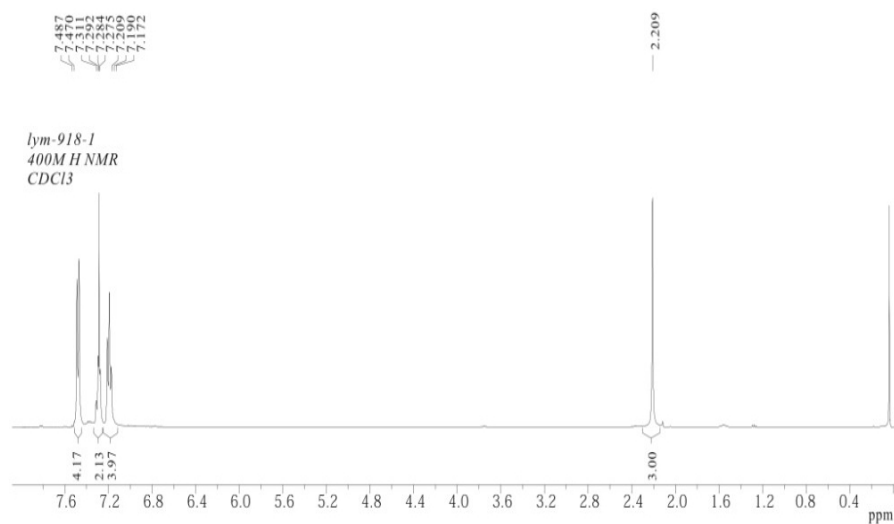


Figure S5a. ^1H NMR spectrum of $[\text{Ag}(\text{MePh}_2\text{pz})]_3 \cdot 1/2\text{CHCl}_3$ (**5**) in CDCl_3 .

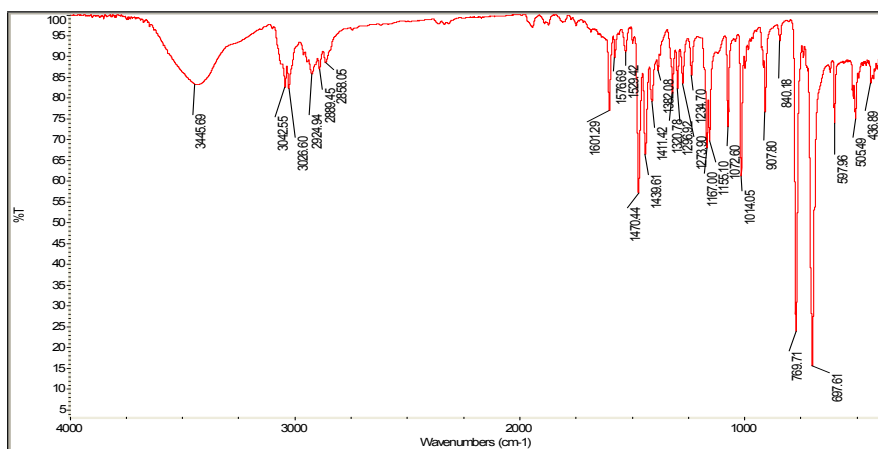


Figure S5b. IR spectra of $[\text{Ag}(\text{MePh}_2\text{pz})]_3 \cdot 1/2\text{CHCl}_3$ (**5**) in KBr pellet.

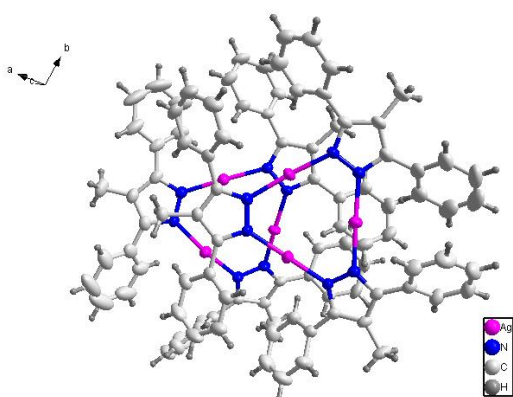


Figure S5c. The asymmetric unit of $[\text{Ag}(\text{MePh}_2\text{pz})]_3 \cdot 1/2\text{CHCl}_3$ (**5**).

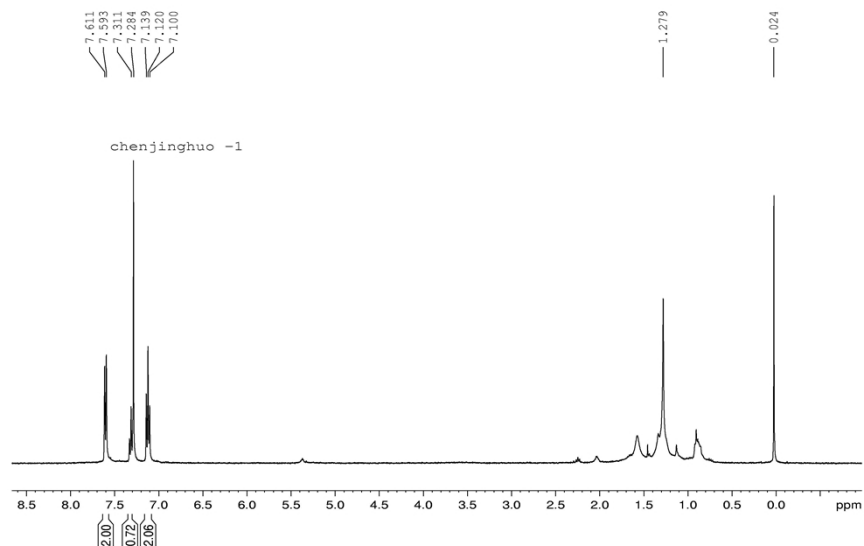


Figure S6a. ^1H NMR spectrum of $[\text{Au}(\text{ClPh}_2\text{pz})]_3 \cdot \text{CH}_2\text{Cl}_2$ (**6**) in CDCl_3 .

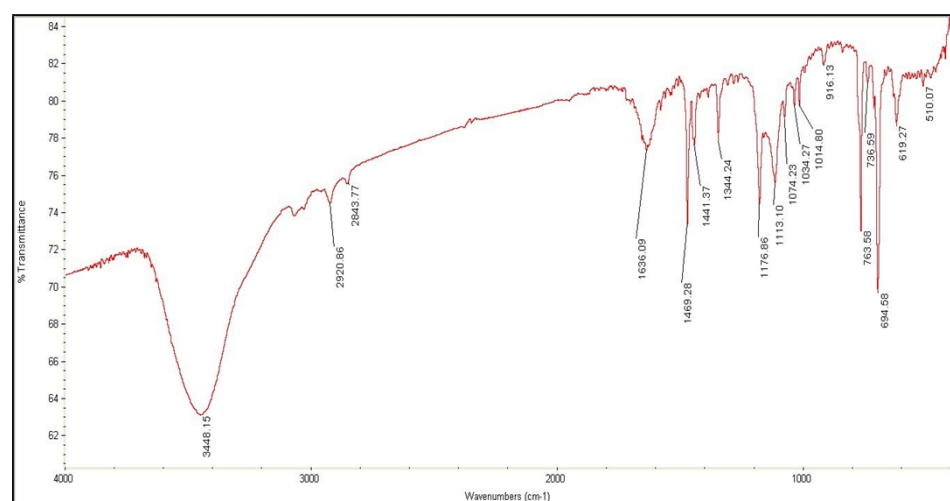


Figure S6b. IR spectrum of $[\text{Au}(\text{ClPh}_2\text{pz})]_3 \cdot \text{CH}_2\text{Cl}_2$ (**6**) in KBr pellet.

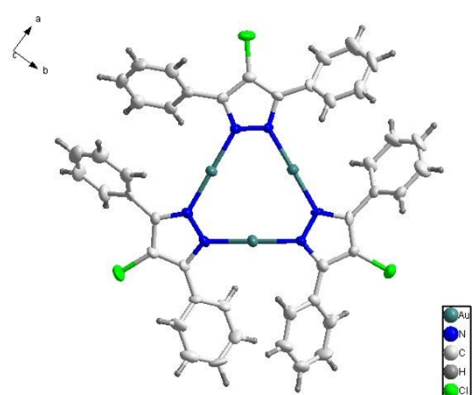


Figure S6c. The asymmetric unit of $[\text{Au}(\text{ClPh}_2\text{pz})]_3 \cdot \text{CH}_2\text{Cl}_2$ (**6**).

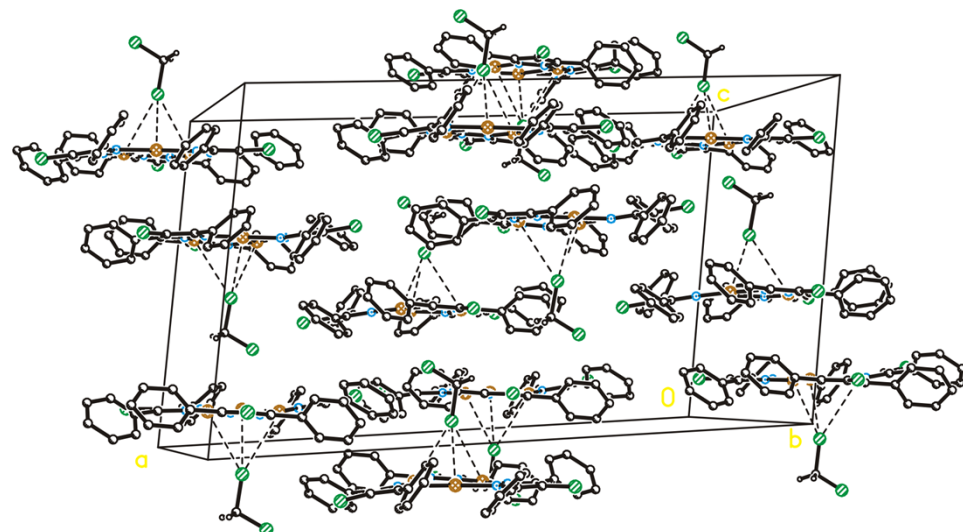


Figure S6d. Packing diagram of $[\text{Au}(\text{ClPh}_2\text{pz})]_3 \cdot \text{CH}_2\text{Cl}_2$ (**6**).

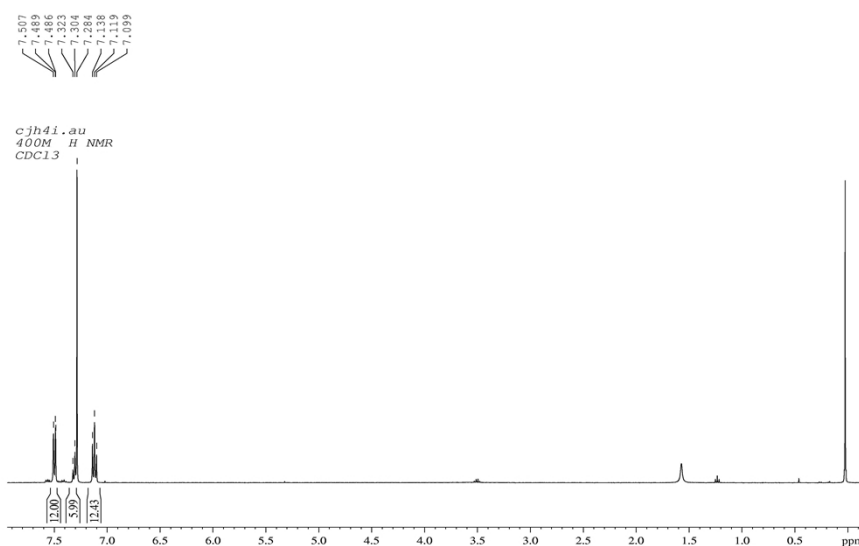


Figure S7a. ^1H NMR spectrum of $[\text{Au}(\text{IPh}_2\text{pz})]_3$ (**7**) in CDCl_3 .

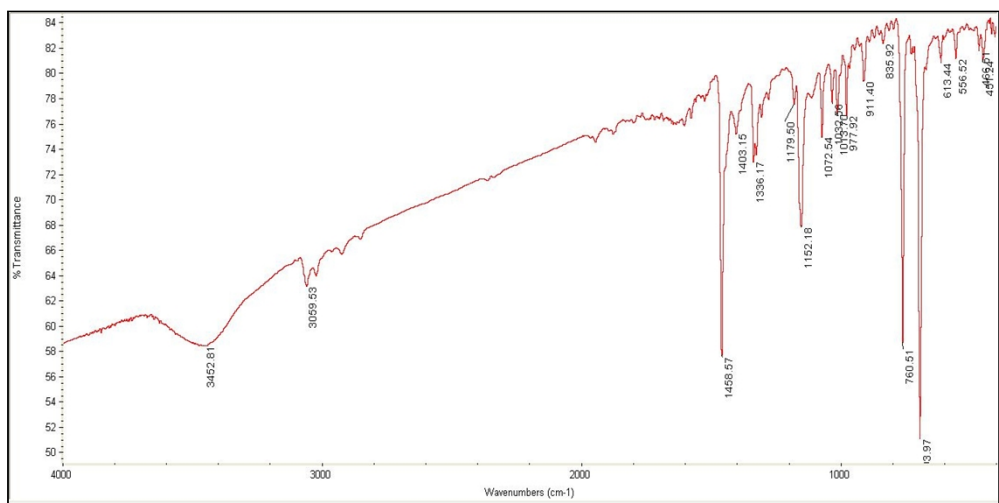


Figure S7b. IR spectrum of $[\text{Au}(\text{IPh}_2\text{pz})]_3$ (**7**) in KBr pellet.

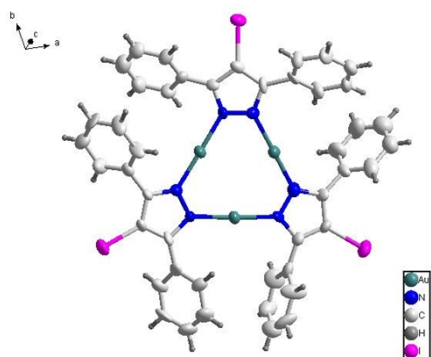


Figure S7c. The asymmetric unit of $[\text{Au}(\text{IPh}_2\text{pz})]_3$ (**7**).

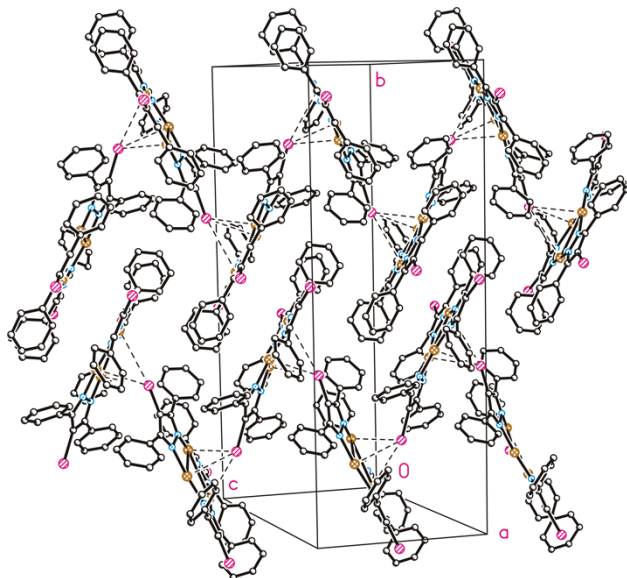


Figure S7d Packing diagram of $[\text{Au}(\text{IPh}_2\text{pz})]_3$ (**7**).

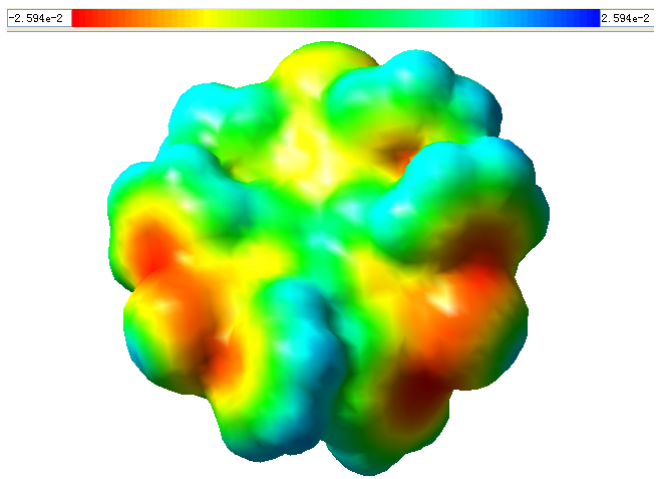


Figure S8a. Top view of MEP surface of $[\text{Ag}(\text{IPh}_2\text{pz})_3]$. MEP color scale is such that the electron density increases from blue → green → yellow → orange → red.

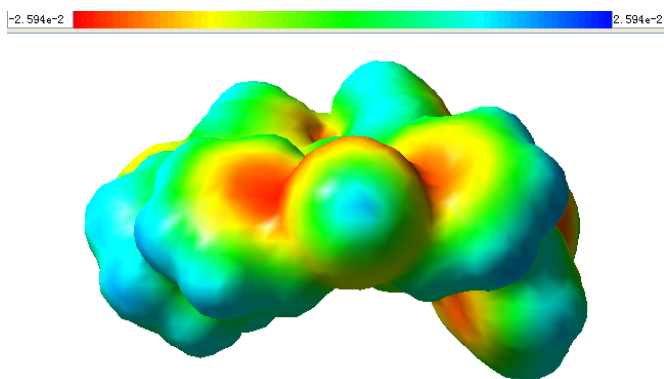


Figure S8b. Side view of MEP surface of $[\text{Ag}(\text{IPh}_2\text{pz})_3]$.

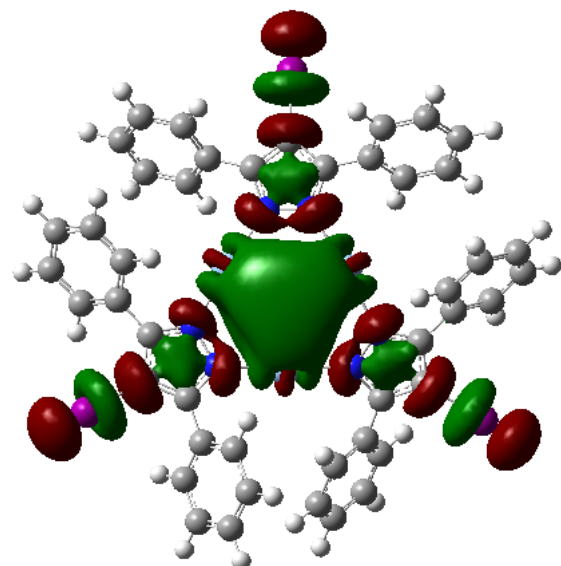


Figure S8c. Top view of LUMO of $[\text{Ag}(\text{IPh}_2\text{pz})_3]$.

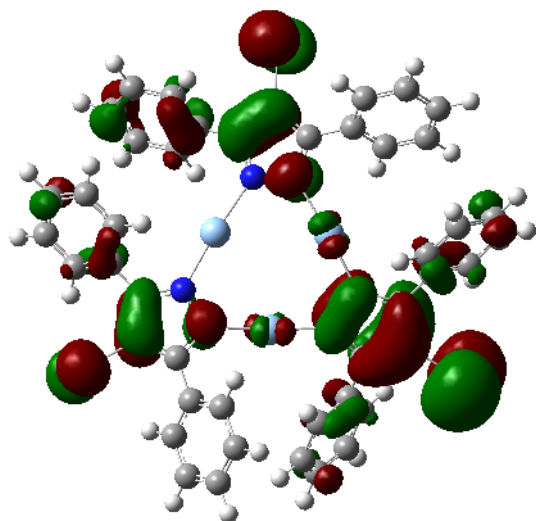


Figure S8d. Top view of HOMO of $[\text{Ag}(\text{IPh}_2\text{pz})]_3$.

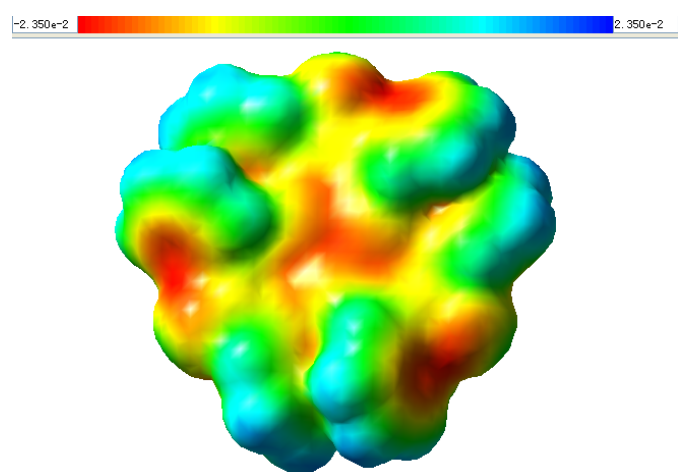


Figure S9a Top view of MEP surface of $[\text{Au}(\text{ClPh}_2\text{pz})]_3$.

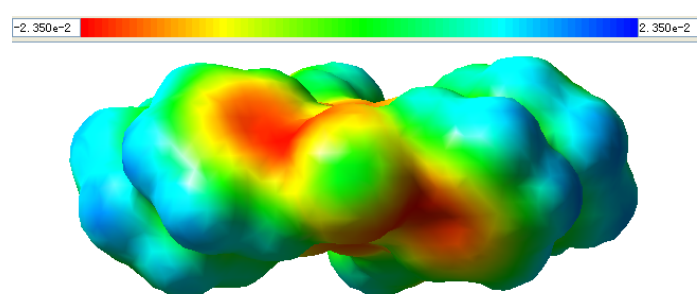


Figure S9b. Side view of MEP surface of $[\text{Au}(\text{ClPh}_2\text{pz})]_3$.

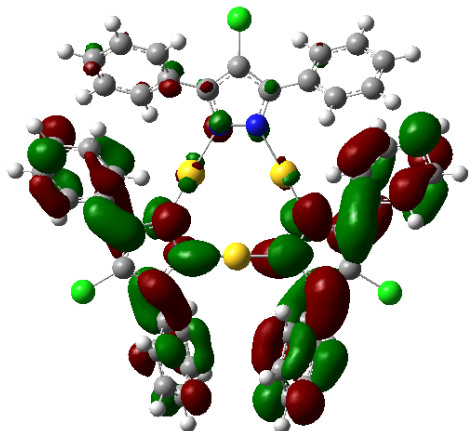


Figure S9c. Top view of LUMO of $[\text{Au}(\text{ClPh}_2\text{pz})]_3$.

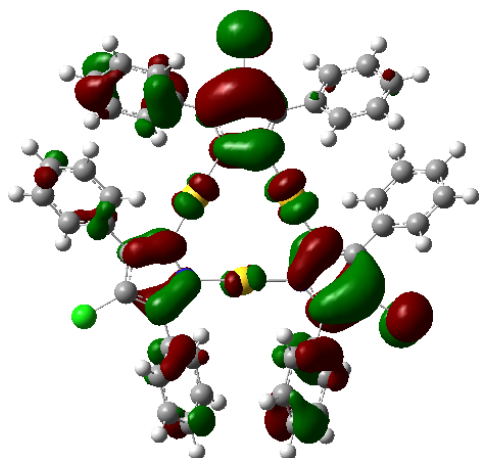


Figure S9d. Side view of HOMO of $[\text{Au}(\text{ClPh}_2\text{pz})]_3$.

Table S1. Selected bond distances (\AA) and bond angles($^{\circ}$).

1			
Ag(1)-N(1)	2.078(2)	Ag(2)-N(3)	2.0914(22)
Ag(1)-N(6)	2.0770(22)	Ag(3)-N(4)	2.0922(25)
Ag(2)-N(2)	2.0849(22)	Ag(3)-N(5)	2.0957(24)
Ag(1)…Ag(2)	3.4195(11)	Ag(1)…N(7)	3.0030(44)
Ag(2)…Ag(3)	3.4852(12)	Ag(3)…N(7)	2.9760(43)
Ag(1)…Ag(3)	3.4711(13)	Ag(2)…N(7)	2.9391(52)
N(1)-Ag(1)-N(6)	175.77(10)	N(2)-Ag(2)-N(3)	173.65(10)
N(4)-Ag(3)-N(5)	173.84(10)		
2			
Ag(1)-N(1)	2.083(11)	Ag(2)-N(3)	2.084(12)
Ag(1)-N(6)	2.091(10)	Ag(3)-N(4)	2.094(11)
Ag(2)-N(2)	2.087(13)	Ag(3)-N(5)	2.113(11)
Ag(1)…Ag(2)	3.5493(16)	Ag(1)…Cl(5)	3.4000(58)
Ag(2)…Ag(3)	3.4813(15)	Ag(2)…Cl(5)	3.4782(68)
Ag(1)…Ag(3)	3.4694(17)	Ag(3)…Cl(7)	3.4342(65)
N(1)-Ag(1)-N(6)	175.9(5)	N(4)-Ag(3)-N(5)	175.5(4)
N(3)-Ag(2)-N(2)	177.8(5)		
3			
Ag(1)-N(1)	2.101(5)	Ag(2)-N(3)	2.088(5)
Ag(1)-N(6)	2.107(5)	Ag(3)-N(4)	2.087(5)
Ag(2)-N(2)	2.090(5)	Ag(3)-N(5)	2.082(5)
Ag(1)…Ag(2)	3.4082(9)	Ag(1)…Cl(1a)	3.4405(18)
Ag(2)…Ag(3)	3.4707(9)	Ag(2)…Cl(1a)	3.4399(18)
Ag(1)…Ag(3)	3.6077(8)	Ag(3)…Cl(1a)	3.1850(17)
N(1)-Ag(1)-N(6)	174.80(19)	N(3)-Ag(2)-N(2)	178.13(19)
N(5)-Ag(3)-N(4)	175.43(19)		

4			
Ag(1)-N(1)	2.081(6)	Ag(2)-N(3)	2.079(5)
Ag(1)-N(6)	2.093(5)	Ag(3)-N(4)	2.088(5)
Ag(2)-N(2)	2.074(5)	Ag(3)-N(5)	2.090(5)
Ag(1)···Ag(2)	3.5957(11)	Ag(1)···I(2a)	3.389(1)
Ag(2)···Ag(3)	3.4763(10)	Ag(2)···I(2a)	3.8178(10)
Ag(1)···Ag(3)	3.4144(12)	Ag(3)···I(2a)	3.6357(13)
N(1)-Ag(1)-N(6)	173.6(2)	N(4)-Ag(3)-N(5)	174.8(2)
N(2)-Ag(2)-N(3)	174.7(2)		
5			
Ag(1)-N(1)	2.087(3)	Ag(4)-N(7)	2.082(3)
Ag(1)-N(6)	2.089(3)	Ag(4)-N(12)	2.092(3)
Ag(2)-N(2)	2.068(3)	Ag(5)-N(8)	2.076(3)
Ag(2)-N(3)	2.059(3)	Ag(5)-N(9)	2.084(3)
Ag(3)-N(4)	2.071(3)	Ag(6)-N(10)	2.073(3)
Ag(3)-N(5)	2.090(3)	Ag(6)-N(11)	2.067(3)
Ag(1)···Ag(2)	3.3683(4)	Ag(4)···Ag(5)	3.4501(1)
Ag(2)···Ag(3)	3.4075(1)	Ag(5)···Ag(6)	3.3417(4)
Ag(1)···Ag(3)	3.5718(1)	Ag(4)···Ag(6)	3.5728(1)
N(1)-Ag(1)-N(6)	175.77(10)	N(7)-Ag(4)-N(12)	173.934(3)
N(2)-Ag(2)-N(3)	173.65(10)	N(8)-Ag(5)-N(9)	175.948(3)
N(4)-Ag(3)-N(5)	173.84(10)	N(10)-Ag(6)-N(11)	174.601(3)
6			
Au(1)-N(1)	2.006(7)	Au(2)-N(3)	2.009(6)
Au(1)-N(6)	2.007(7)	Au(3)-N(4)	1.997(7)
Au(2)-N(2)	1.999(6)	Au(3)-N(5)	2.006(7)
Au(1)···Au(2)	3.3396(5)	Au(1)···Cl(4)	3.5898(35)
Au(2)···Au(3)	3.3642(5)	Au(3)···Cl(4)	3.5948(31)

